Jan IŻYKOWSKI, Eugeniusz ROSOŁOWSKI, Piotr PIERZ

Wrocław University of Technology

doi:10.15199/48.2016.07.17

Location of complex faults on overhead power line

***Abstract**. One-end algorithm for locating an open conductor failure combined with an earth fault on power lines has been presented. Two cases: an open conductor failure occurring in front of and behind an earth fault, respectively, have been considered. The sample case with the fault data obtained from ATP-EMTP simulation is included and discussed.*

***Streszczenie.** Przedstawiono algorytm do lokalizowania przerwy w przewodzie występującej wraz ze zwarciem doziemnym w napowietrznych liniach elektro-energetycznych, z użyciem pomiarów z jednego końca linii. Rozpatrzono dwa przypadki: przerwa odpowiednio przed i za zwarciem doziemnym. Zamieszczono przykład z zastosowaniem sygnałów z symulacji z pomocą programu ATP-EMTP i przeprowadzono dyskusję rezultatów. (**Lokalizowanie zwarć złożonych w napowietrznej linii elektro-energetycznej**).*

Keywords: power line, open conductor failure, earth fault, fault location, computer simulation.
Słowa kluczowe: linia elektro-energetyczna, przerwa w przewodzie, zwarcie doziemne, lokalizacja zwarcia, symulacja komputerowa.

Introduction

Fault statistics unambiguously indicate that majority of total number of power system faults occur on overhead power lines. Such faults have to be detected [1] and then located by protective relays (operating in on-line mode) as well as by fault locators (operating in off-line mode) which are considered in this paper.

Varieties of one-end fault location impedance-based algorithms for fault locators have been developed so far [2]–[5]. Three-phase current $\{i_a, i_b, i_c\}$ and voltage $\{v_a, v_b, v_c\}$ acquired at one end of the line, from the phases: a, b, c, are considered as such fault locator (FL) input signals (Fig. 1). The aim of the FL is to determine a distance to fault: d, expressed within this paper in per units [p.u.]. The already known algorithms [2]–[5] differ in many aspects, however, all of them are designed for locating typical shunt faults: single phase-to-earth (as in Fig. 2b), phase-to-phase, phase-to-phase-to-earth and three phase faults.

This paper, in turn, is focused on locating complex faults in a form of an open conductor failure combined with a phase-to earth fault – Fig. 2 [6]. Such fault results from a mechanical failure of a phase conductor, with one of the break coming into contact with earth. As so far, there are no available statistics for such faults.

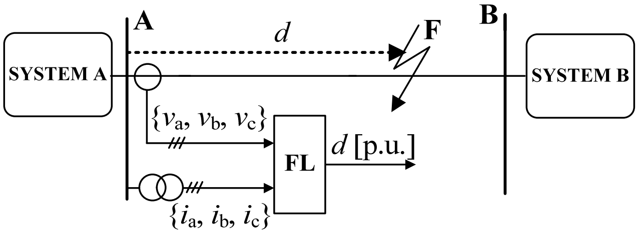

Fig. 1. Principle of one-end fault location

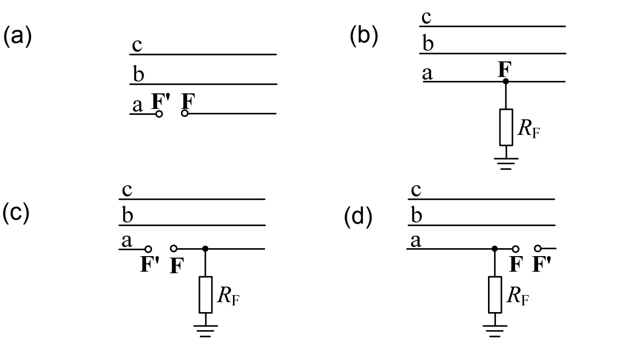

Fig. 2. Models of different faults: (a) open conductor failure alone (b) single phase-to-earth fault alone, (c) open conductor failure in front of earth fault, (d) open conductor failure behind earth fault

The complex faults being a combination of earth fault with open conductor failure have been considered in not numerous publications. In particular, such faults have been studied in relation to their simulation [7], calculation [8]–[9] and protection [10]–[12]. In turn, fault location of such faults was considered in [6], while this paper continues this research.

When considering the complex faults, two different sequences of an earth fault and an open conductor failure, as shown in Fig. 2c and d, have been considered. The algorithm for locating the complex faults has been derived with using the generalised fault loop model [3]. For evaluating this algorithm, the fault data obtained from versatile ATP-EMTP [13] simulations of faults have been applied.

Fault location algorithm

Overall structure for locating both the typical shunt faults and the considered here complex faults [6] is presented in Fig. 3.

Firstly, an occurred fault has to be detected and then it undergoes classification, in terms which phases are taking part in a fault and whether earth is involved or not. Then, both typical and complex faults are to be located. Finally, selection of the valid result has to be carried out or two alternative results are yielded (Fig. 3).

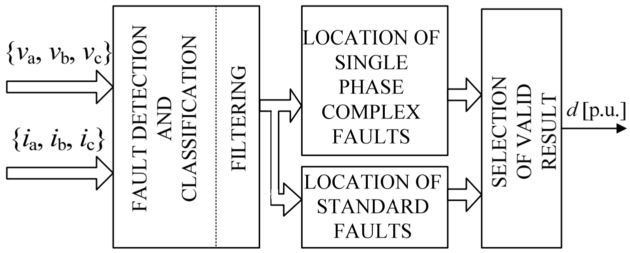

Fig. 3. Overall structure for locating typical and complex faults on power line

The considered fault location algorithm is stated in terms of symmetrical components (Fig. 4) by applying the generalised fault loop model described in [3].

Fig. 4 presents equivalent circuit diagrams of the transmission network for particular sequences (positive-, incremental positive-, negative- and zero-sequence) under an earth fault appearing behind an open conductor failure (as in Fig. 2c). The circuit diagrams for the other case (as in Fig. 2d) are formed analogously. It is assumed that impedances for the negative- and the positive-sequence are identical.

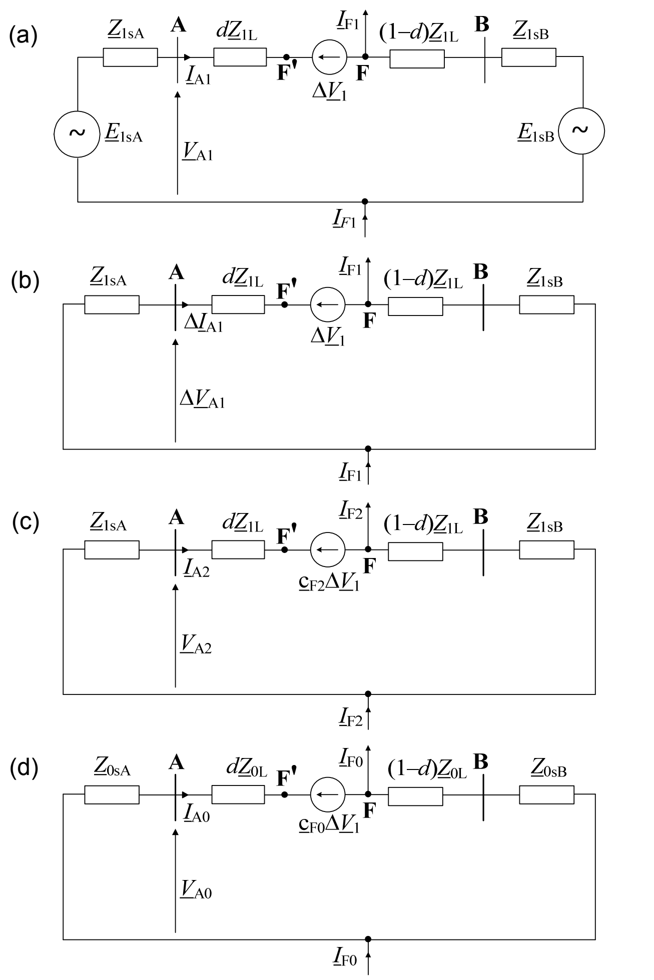

Fig. 4. The case of open conductor failure in front of earth fault – equivalent circuit diagrams of the transmission network for: (a) positive-sequence, (b) incremental positive-sequence, (c) negative-sequence, (d) zero-sequence

In order to derive the fault location algorithm covering both the cases of Fig. 2 with respect to sequences of the open conductor failure and the earth fault, the following generalised fault loop model [3] is proposed:

(1) $$\underline{V}_{A\_p} - d\underline{Z}_{1L}\underline{I}_{A\_p} - \underline{P}\Delta\underline{V}_1 - R_F\sum_{i=0}^{2}\underline{a}_{Fi}\underline{I}_{Fi} = 0$$

where: d – sought distance to fault (p.u.), R_F – fault resistance, $\Delta\underline{V}_1$ – voltage drop across open conductor failure for positive sequence,

$\underline{V}_{A\_p} = \underline{a}_1\underline{V}_{A1} + \underline{a}_2\underline{V}_{A2} + \underline{a}_0\underline{V}_{A0}$ – fault loop voltage,

$\underline{I}_{A\_p} = \underline{a}_1\underline{I}_{A1} + \underline{a}_2\underline{I}_{A2} + \underline{a}_0(\underline{Z}_{0L}/\underline{Z}_{1L})\underline{I}_{A0}$ – fault loop current,

$\underline{a}_1$, $\underline{a}_2$, $\underline{a}_0$ – weighting coefficients dependent on fault type used for composing fault loop signals, identically as for the distance protection (Table 1),

$\underline{a}_{F1}$, $\underline{a}_{F2}$, $\underline{a}_{F0}$ – share coefficients dependent on fault type and preference for using the sequences (Table 2),

$\underline{Z}_{1L}$, $\underline{Z}_{0L}$ – impedance of a line for positive (negative) and for zero sequences,

$\underline{P} = \underline{a}_1 + \underline{a}_2\underline{c}_{F2} + \underline{a}_0\underline{c}_{F0}$ – for the case of Fig. 2c,

$\underline{P} = 0$ – for the case of Fig. 2d.

Table 1. Weighting coefficients for determining fault loop voltage and current

Faulted Phase:	$\underline{a}_1$	$\underline{a}_2$	$\underline{a}_0$
a	1	1	1
b	$\underline{a}^2$	$\underline{a}$	1
c	$\underline{a}$	$\underline{a}^2$	1
$\underline{a} = \exp(j2\pi/3)$, $j = \sqrt{-1}$			

Table 2. Coefficients used in (1)–(4)

Fault	$\underline{a}_{F2}$	$\underline{b}_{F1}$	$\underline{b}_{F2}$	$\underline{c}_{F1}$	$\underline{c}_{F2}$
(a-E)&a open	3	0	1	1	1
(b-E)&b open	$3\underline{a}$	0	$\underline{a}$	$\underline{a}$	$\underline{a}^2$
(c-E)&c open	$3\underline{a}^2$	0	$\underline{a}^2$	$\underline{a}^2$	$\underline{a}$
	$\underline{a}_{F1}=\underline{a}_{F0}=\underline{c}_{F0}=0$; $\underline{a}=\exp(j2\pi/3)$; $j=\sqrt{-1}$				

Taking for further analysis the recommended set of the share coefficients from Table 2,, the generalised fault loop model becomes:

(2) $$\underline{V}_{A\_p} - d\underline{Z}_{1L}\underline{I}_{A\_p} - \underline{P}\Delta\underline{V}_1 - R_F\underline{a}_{F2}\underline{I}_{F2} = 0$$

Thus, there are four unknowns: d, R_F, $\Delta\underline{V}_1$ and $\underline{I}_{F2}$ in (2) under availability of one-end measurements only. The model (2) is not directly solvable and thus one needs to formulate additional equations to provide sufficient number of equations with respect to the specified unknowns in (2). For this purpose the flow of currents in the equivalent circuit diagrams of Fig. 4c and Fig. 4d has been considered. As a result, the negative and zero sequences of the total fault current (fault path current) are determined as follows:

(3) $$\underline{I}_{F2} = \frac{(\underline{Z}_{1sA} + \underline{Z}_{1L} + \underline{Z}_{1sB})\underline{I}_{A2} + \underline{c}_{F2}\Delta\underline{V}_1}{-\underline{Z}_{1L}d + (\underline{Z}_{1L} + \underline{Z}_{1sB})}$$

(4) $$\underline{I}_{F0} = \frac{(\underline{Z}_{0sA} + \underline{Z}_{0L} + \underline{Z}_{0sB})\underline{I}_{A0} + \underline{c}_{F0}\Delta\underline{V}_1}{-\underline{Z}_{0L}d + (\underline{Z}_{0L} + \underline{Z}_{0sB})}$$

To enable solution of (2), additionally the relation between the sequence components of the total fault current [3] is utilised:

(5) $$\underline{I}_{F0} = \underline{b}_{F1}\underline{I}_{F1} + \underline{b}_{F2}\underline{I}_{F2}$$

where the recommended coefficients $\underline{b}_{F1}$, $\underline{b}_{F2}$ are gathered in Table 2.

Substitution of (3) and (4) into (5) yields:

(6) $$\Delta\underline{V}_1 = \frac{(\underline{Q}_1\underline{I}_{A2} + \underline{Q}_2\underline{I}_{A0})d + (\underline{Q}_3\underline{I}_{A2} + \underline{Q}_4\underline{I}_{A0})}{\underline{Q}_5 d + \underline{Q}_6}$$

where:

$\underline{Q}_1 = \underline{Z}_{0L}\underline{b}_{F2}(\underline{Z}_{1sA} + \underline{Z}_{1L} + \underline{Z}_{1sB})$,

$\underline{Q}_2 = -\underline{Z}_{1L}(\underline{Z}_{0sA} + \underline{Z}_{0L} + \underline{Z}_{0sB})$,

$\underline{Q}_3 = -\underline{b}_{F2}(\underline{Z}_{0L} + \underline{Z}_{0sB})(\underline{Z}_{1sA} + \underline{Z}_{1L} + \underline{Z}_{1sB})$,

$\underline{Q}_4 = (\underline{Z}_{1L} + \underline{Z}_{1sB})(\underline{Z}_{0sA} + \underline{Z}_{0L} + \underline{Z}_{0sB})$,

$\underline{Q}_5 = \underline{c}_{F0}\underline{Z}_{1L} - \underline{b}_{F2}\underline{c}_{F2}\underline{Z}_{0L}$,

$\underline{Q}_6 = \underline{b}_{F2}\underline{c}_{F2}(\underline{Z}_{0L} + \underline{Z}_{0sB}) - \underline{c}_{F0}(\underline{Z}_{1L} + \underline{Z}_{1sB})$.

In turn, substitution of (6) into (3) gives the formula for the negative-sequence component of the fault path current:

(7) $$\underline{I}_{F2} = \frac{(\underline{Q}_7 \underline{I}_{A2} + \underline{Q}_8 \underline{I}_{A0})d + (\underline{Q}_9 \underline{I}_{A2} + \underline{Q}_{10} \underline{I}_{A0})}{\underline{Q}_{11} d^2 + \underline{Q}_{12} d + \underline{Q}_{13}}$$

where:

$\underline{Q}_7 = (\underline{Z}_{1sA} + \underline{Z}_{1L} + \underline{Z}_{1sB})\underline{Q}_5 + \underline{c}_{F2}\underline{Q}_1$,

$\underline{Q}_8 = \underline{c}_{F2}\underline{Q}_2$,

$\underline{Q}_9 = (\underline{Z}_{1sA} + \underline{Z}_{1L} + \underline{Z}_{1sB})\underline{Q}_6 + \underline{c}_{F2}\underline{Q}_3$,

$\underline{Q}_{10} = \underline{c}_{F2}\underline{Q}_4$,

$\underline{Q}_{11} = -\underline{Z}_{1L}\underline{Q}_5$,

$\underline{Q}_{12} = (\underline{Z}_{1L} + \underline{Z}_{1sB})\underline{Q}_5 - \underline{Q}_6\underline{Z}_{1L}$,

$\underline{Q}_{13} = \underline{Q}_6(\underline{Z}_{1L} + \underline{Z}_{1sB})$.

All the coefficients ($\underline{Q}_1 \div \underline{Q}_{13}$) involved in (6)–(7) are determined by the parameters of the equivalent circuit diagrams (Fig. 4) and the coefficients dependent on fault type coefficients (Table 2). By expressing the unknowns $\Delta\underline{V}_1$ and $\underline{I}_{F2}$ as the functions of the sought distance to fault: (*d*) – as in (6) and (7), the fault location problem reduces to solving the fault loop model (2) with only two unknowns: d [p.u.] – distance to fault and R_F – fault path resistance, thus, analogously as in the other one-end fault location algorithms [3].

Results

In order to illustrate behaviour of the derived algorithm, the ATP-EMTP software package [13] has been used to simulate variety of fault cases on the transmission line of 400 kV, 300 km, and the selected results are shown in Figs. 5, 6 and 7. Data for the transmission line (impedances and capacitances) and impedances of the equivalent systems (sources) were assumed as:

$\underline{Z}_{1L} = (0.0275 + 0.31513\mathrm{j})\ \Omega/\mathrm{km}$,

$\underline{Z}_{0L} = (0.275 + 1.0265\mathrm{j})\ \Omega/\mathrm{km}$,

$C_{1L} = 13.0\ \mathrm{nF/km}$, $C_{0L} = 8.5\ \mathrm{nF/km}$,

$\underline{Z}_{1sA} = (1.312 + 15\,\mathrm{j})\ \Omega$, $\underline{Z}_{0sA} = (2.334 + 26.6\,\mathrm{j})\ \Omega$,

$\underline{Z}_{1sB} = 2\underline{Z}_{1sA}$, $\underline{Z}_{0sB} = 2\underline{Z}_{0sA}$.

The case of the open conductor failure in front of the earth fault (results shown in Fig. 5) appears as much more difficult for locating. This is due to gross distortion of the fault locator input signals. Phase currents are grossly distorted with the oscillatory components appearing as a result of flow of the faulted phase current through the shunt capacitances of the line only. The cascade filtration of the signals has been applied. The sine half cycle filter has been used in the 1st stage of the cascade, while the pair of orthogonal full cycle Fourier filters in the 2nd stage. Fault location accuracy for the opposite case of open conductor failure behind the earth fault (Fig. 6) is generally better.

The sample results of fault location accuracy evaluation are shown in Fig. 7a and b. The faults were applied at different locations and the involved fault resistance was: R_F=10 Ω. For the case of the broken conductor failure in front of the ground fault (Fig. 7a) the error can reach around 3%, while for the opposite case (as presented in Fig. 7b) much better accuracy is provided and the error does not exceed 1%. Such level of errors is kept for fault resistances up to the range of 25 Ω.

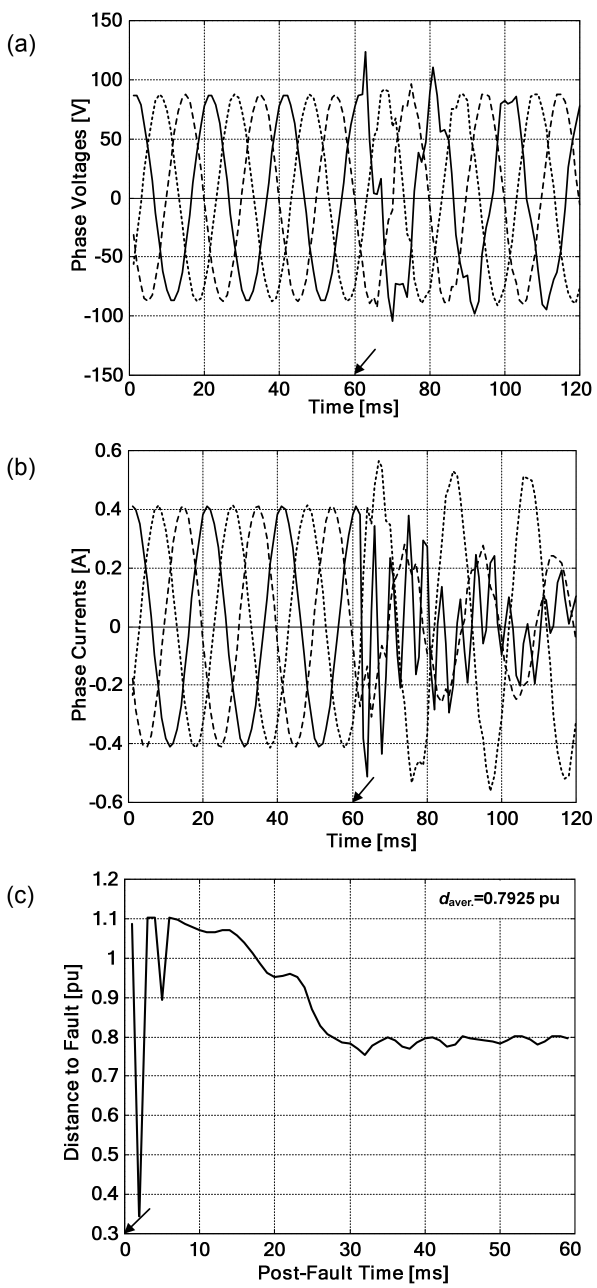

Fig. 5. Example of fault location – open conductor failure in front of a-E fault, R_F=10 Ω, d=0.8 p.u.: (a) secondary phase voltages, (b) secondary phase currents, (c) distance to fault

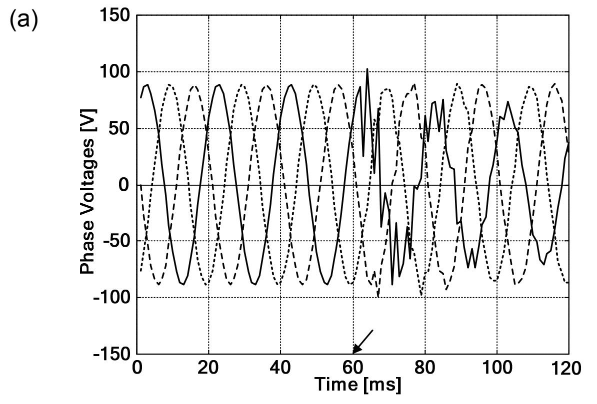

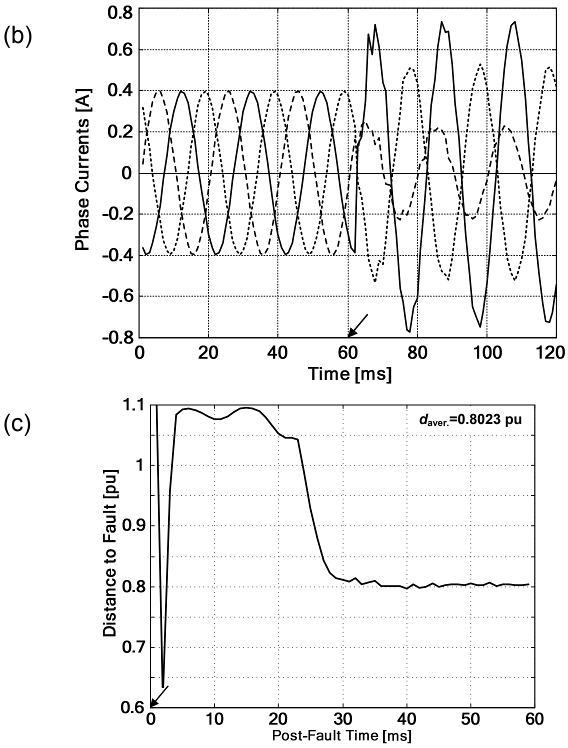

Fig. 6. Example of fault location – open conductor failure behind a-E fault, R_F=10 Ω, d=0.8 p.u.: (a) secondary phase voltages, (b) secondary phase currents, (c) distance to fault

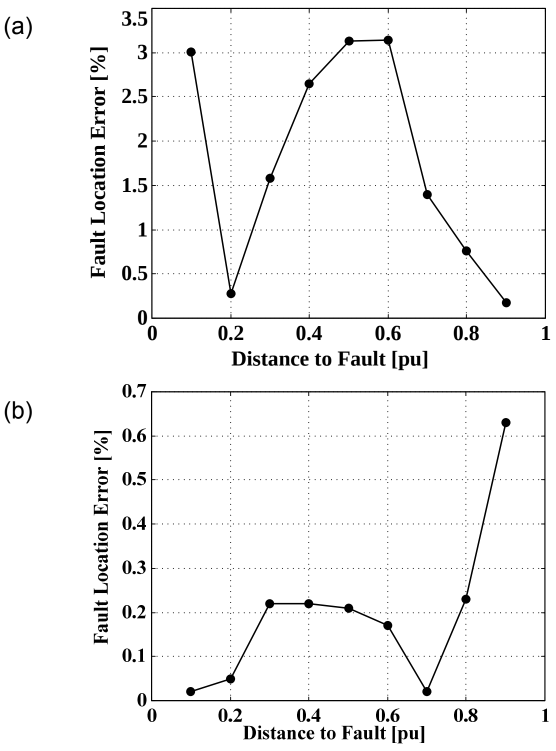

Fig. 7. Errors for locating broken conductor failure occurring: (a) in front of a-E fault, (b) behind a-E fault

Conclusions

Efficient one-end algorithm for locating earth fault combined with an open conductor failure has been presented. Different sequences for appearing the earth fault and the open conductor failure, namely the open conductor failure in front of and behind the phase-to-earth fault, have been taken into account. Generalised models of fault loops and faults have been applied for formulation of the algorithm. The presented approach can be incorporated into two-end fault location methods, which at present do not offer the possibilities for locating the complex faults considered in this paper.

The developed fault location algorithm has been evaluated with use of the fault data obtained from versatile ATP-EMTP simulations. The attached examples show satisfactory performance of the algorithm. Certain poor accuracy of fault location is observed for open conductor failure in front of the earth fault. Improvement of accuracy for these cases requires incorporating more sophisticated filtering of the input signals and including the compensation for shunt capacitances of a line.

Authors: *prof. dr hab. inż. Jan Iżykowski, prof. dr hab. inż. Eugeniusz Rosołowski, dr inż. Piotr Pierz; Politechnika Wrocławska, Katedra Energoelektryki, ul. Wybrzeże Wyspiańskiego 27, 50-370 Wrocław; E-mails: jan.izykowski@pwr.edu.pl; eugeniusz.rosolowski@pwr.edu.pl; piotr.pierz@pwr.edu.pl.*

REFERENCES

[1] Ferraz R.G., Iurinic L.U., Filomena A., Bretas A., Park's transformation based formulation for power systems transients detection, *Journal of Present Problems of Power System Control, Scientific Papers of the Department of Electrical Power Engineering of Wroclaw University of Technology*, Autumn 2013, pp. 5–23, ISSN 2084-2201, http://www.psc.pwr.wroc.pl
[2] IEEE Std C37.114: IEEE Guide for Determining Fault Location on AC Transmission and Distribution Lines, *IEEE Power Engineering Society Publ.,* pp. 1–42, 2005
[3] Saha M.M., Izykowski J., Rosolowski E., *Fault Location on Power Networks*, Springer, London 2010
[4] Eriksson L., Saha M.M., Rockefeller G.D., An accurate fault locator with compensation for apparent reactance in the fault resistance resulting from remote-end infeed, *IEEE Trans. on PAS*, vol. PAS-104, No.2, 1985, pp. 424-436
[5] Wiszniewski A., Dokładna lokalizacja miejsca zwarcia w liniach napowietrznych elektroenergetycznych, *Przegląd Elektrotechniczny*, 1984, R. 60, nr 2, pp. 41-44
[6] Izykowski J., Rosolowski E., Pierz P., Location of open conductor failure combined with phase-to-earth fault on power line, *Proceedings of 2015 16th International Conference on Computational Problems of Electrical Engineering (CPEE),* Lviv, Ukraine, September 2–5, 2015, pp. 56–58
[7] Smith D.R., Digital simulation of simultaneous unbalances involving open and faulted conductors, *IEEE Trans. on PAS*, VOL. PAS-89, NO. 8, 1970, pp. 1826–1825.
[8] Roy L., Rao N.D., Exact calculation of simultaneous faults involving open conductors and line-to-ground short circuits on inherently unbalanced power systems, *IEEE Trans. on PAS*, Vol. PAS-101, No. 8 August 1982, pp. 2738–2746.
[9] Abouelenin F.M., A complete algorithm to fault calculation due to simultaneous faults: combination of short circuits and open lines, Proceedings of JEEIE MELECON 2002, May 7-9, 2002, Cairo, Egypt, pp. 522–526
[10] Cook V., *Analysis of distance protection*, Research Study Press Ltd., John Wiley & Sons Inc., 1985
[11] Makwana V.H., Bhalja B.R., A new digital distance relaying scheme for series-compensated double-circuit line during open conductor and ground fault, *IEEE Trans. on Power Delivery*, vol. 27, no. 2, April 2012, pp. 910–917
[12] Razaz M., Seifossadat S.G., Razaz M., Joorabian M., A digital ground distance relaying algorithm to reduce the effect of fault resistance during single phase to ground and simultaneous faults, *Majlesi Journal of Electrical Engineering*, Vol. 9, No. 1, March 2015, pp. 85–92
[13] Dommel H., *ElectroMagnetic Transients Program*, BPA, Portland, Oregon, 1986.